

## THERMAL ANALYSIS OF SOME POLYNUCLEAR COORDINATION COMPOUNDS AS PRECURSORS OF IRON GARNETS ( $M_3Fe_5O_{12}$ , $M=Y^{3+}$ or $Er^{3+}$ )

Luminita Patron<sup>1</sup>, Oana Carp<sup>1,\*</sup>, I. Mindru<sup>1</sup>, G. Marinescu<sup>1</sup>, J. Hanss<sup>2</sup> and A. Reller<sup>2</sup>

<sup>1</sup>Ilie Murgulescu' Institute of Physical Chemistry, Spl. Independentei 202, sect.6, 060021 Bucharest, Romania

<sup>2</sup>Solid State Chemistry, University of Augsburg, Universitätsstrasse 1, 86159 Augsburg, Germany

The thermal behaviour of four coordination compounds  $(NH_4)_6[Y_3Fe_5(C_4O_5H_4)_6(C_4O_5H_3)_6] \cdot 12H_2O$ ,  $(NH_4)_6[Y_3Fe_5(C_6O_7H_{10})_6(C_6O_7H_9)_6] \cdot 8H_2O$ ,  $(NH_4)_6[Er_3Fe_5(C_4O_5H_4)_6(C_4O_5H_3)_6] \cdot 10H_2O$  and  $(NH_4)_6[Er_3Fe_5(C_4O_6H_4)_6(C_4O_6H_3)_6] \cdot 22H_2O$  has been studied to evaluate their suitability for garnet synthesis. The thermal decomposition and the phase composition of the resulted decomposition compounds are influenced by the nature of metallic cations (yttrium-iron or erbium-iron) and ligand anions ( malate or gluconate).

**Keywords:** coordination compounds, garnets, precursors, thermal analysis

### Introduction

In the last years, the use of coordination compounds as sources of mixed oxides has expanded [1–3]. The decomposition processes of various metal carboxylates under heating were widely studied. The simplest compounds like formates and oxalates were scrutinized; the compounds containing as ligands anions of polyhydroxy carboxylic, aromatic and unsaturated carboxylic acids were also investigated [4–12].

In this paper we report the thermal behaviour of four polynuclear coordination compounds containing as ligands malate and gluconate anions, potential precursors of yttrium and erbium garnets ( $M_3Fe_5O_{12}$ ,  $M=Y^{3+}$  or  $Er^{3+}$ ), emphasizing the influence of the complexing agent on the thermal behaviour of the precursor and implicit on mixed oxides properties.

### Experimental

As raw materials in the synthesis of precursors,  $Fe(NO_3)_3 \cdot 9H_2O$ ,  $Y_2O_3$ ,  $Er_2O_3$ , malic acid and  $\delta$ -gluconolactone of reagent quality (Merck) were used. First, the oxides were converted into nitrates by  $HNO_3$  adding. Afterward, from a solution containing metal nitrates and polyhydroxy carboxylic acid, in a ratio  $M^{3+} - Fe^{3+} - carboxylic\ acid = 3:5:12$  for malic acid and  $3:5:24$  for  $\delta$ -gluconolactone the polynuclear coordination compounds were separated by extraction with ethanol. A complete precipitation required 24 h, time interval in which repeated adjustings of the pH to 5–6 values by addition of a 1:1  $NH_4OH:C_2H_5OH$  solution were

performed. The separated fine light brown precipitates were filtered, washed with ethanol and dried. The compounds were characterized by elemental chemical analysis: the metal content was determined by atomic absorption with a SAA1 device and gravimetric techniques, and the CHN by a Carl Erba Model 1108 CHNS-O elemental analyzer. Four polynuclear coordination compounds were synthesized:  $(NH_4)_6[Y_3Fe_5(C_4O_5H_4)_6(C_4O_5H_3)_6] \cdot 12H_2O$ ,  $(NH_4)_6[Y_3Fe_5(C_6O_7H_{10})_6(C_6O_7H_9)_6] \cdot 8H_2O$ ,  $(NH_4)_6[Er_3Fe_5(C_4O_5H_4)_6(C_4O_5H_3)_6] \cdot 10H_2O$  and  $(NH_4)_6[Er_3Fe_5(C_6O_7H_{10})_6(C_6O_7H_9)_6] \cdot 22H_2O$ . The thermochemical investigations were carried out under dynamic air atmosphere ( $15\text{ cm}^3\text{ min}^{-1}$ ), with sample mass about 40 mg at heating rates of  $5\text{--}20\text{ K min}^{-1}$ . DSC measurements were performed on a Netzsch thermobalance STA 409CC/PG/PC type, while the thermogravimetry/mass spectrometry on a STA 409 C one. The IR spectra ( $400\text{--}4000\text{ cm}^{-1}$ ) were recorded with a BIO-RAD FTIR 125 type spectrophotometer in KBr pellets. The crystalline phases in the calcinated powders were identified by XRD powder methods using a Philips Xpert X-Ray diffractometer ( $CuK_\alpha$  radiation). Diffraction peaks were fitted assuming Voight-function for the peak profile. For the determination of the average crystallites size it has been used the Scherrer formula  $D=0.91\lambda/(\beta\cos\theta)$ , where  $D$  is the crystallite size,  $\lambda$  the wavelength ( $CuK_\alpha$ ),  $\beta$  the corrected half-width obtained using  $\alpha$ -quartz as reference and  $\theta$  the diffraction angle. The transmission microscopy investigations of the obtained oxides were performed on a Philips CM30 device.

\* Author for correspondence: carp@acodarom.ro

## Results and discussion

The isolated coordination compounds are characterized by the molecular formula  $(\text{NH}_4)_6[\text{Y}_3\text{Fe}_5(\text{C}_4\text{O}_5\text{H}_4)_6(\text{C}_4\text{O}_5\text{H}_3)_6]\cdot 12\text{H}_2\text{O}$ ,  $(\text{NH}_4)_6[\text{Y}_3\text{Fe}_5(\text{C}_6\text{O}_7\text{H}_{10})_6(\text{C}_6\text{O}_7\text{H}_9)_6]\cdot 8\text{H}_2\text{O}$ ,  $(\text{NH}_4)_6[\text{Er}_3\text{Fe}_5(\text{C}_4\text{O}_5\text{H}_4)_6(\text{C}_4\text{O}_5\text{H}_3)_6]\cdot 10\text{H}_2\text{O}$  and  $(\text{NH}_4)_6[\text{Er}_3\text{Fe}_5(\text{C}_6\text{O}_7\text{H}_{10})_6(\text{C}_6\text{O}_7\text{H}_9)_6]\cdot 22\text{H}_2\text{O}$ , where  $\text{C}_4\text{O}_5\text{H}_4^{2-}$ ,  $\text{C}_4\text{O}_5\text{H}_3^{3-}$  are malate di- and tri-anions and,  $\text{C}_6\text{O}_7\text{H}_{10}^{2-}$ ,  $\text{C}_6\text{O}_7\text{H}_9^{3-}$ , gluconate di- and tri-anions. In the complexes the metallic ions adopt an octahedral configuration [13, 14]. The anionic ligands are coordinated by both the carboxylic and hydroxyl groups [15]. Details about synthesis and physical-chemical characterization of the coordination compounds are presented elsewhere [16].

### *Yttrium-iron coordination compounds thermal decomposition*

In the temperature range of 331.9–1160.8 K the malate compound  $(\text{NH}_4)_6[\text{Y}_3\text{Fe}_5(\text{C}_4\text{O}_5\text{H}_4)_6(\text{C}_4\text{O}_5\text{H}_3)_6]\cdot 12\text{H}_2\text{O}$  undergoes a stepwise decomposition in five distinct stages of mass loss. The observed mass loss (70.08%) is in good agreement with the calculated one (69.85%). The TG, DSC, DTG and the most representative ion intensities curves corresponding to  $m/z=18$  ( $\text{H}_2\text{O}$ ) and 44 ( $\text{CO}_2$ ) are depicted in Fig. 1.

The first decomposition step (331.9–395.6 K,  $T_{\max \text{DTG}}=359.4$  K) represents the evolving of six  $\text{NH}_3$  and two  $\text{H}_2\text{O}$  molecules (calcd./found: 6.10/5.64%). The second step, (395.6–558.1 K,  $T_{\max \text{DTG}}=450$  K), consists in an overlapping of at least two decomposition steps: the releasing of the remainder outer coordination sphere water molecule and the oxidative degradation of the malate ligand. The formation of an oxoacetate intermediate corresponding to the molecular formula  $[\text{Y}_3\text{Fe}_5\text{O}_8(\text{CH}_3\text{COO})_8]$  may be advanced based on FTIR results (the appearance of absorption peaks at  $\sim 1020$  and  $1050\text{ cm}^{-1}$  attributed to acetate anion [17]) and on the thermogravimetric calculus (calcd./found: 47.73/46.13%). The development of acetate intermediates during the degradative oxidation of malates is already mentioned by literature [18–21]. Rising the temperature, this intermediate decomposes (558.1–661.9 K,  $T_{\max \text{DTG}}=620$  K) leading to an amorphous oxocarbonate, namely  $\text{Y}_3\text{Fe}_5(\text{CO}_3)_3\text{O}_9$  (calcd./found: 11.27/12.75%). The last three decomposition steps (661.9–1160.8 K) represent a stepwise decomposition of the formed oxocarbonate:  $\text{Y}_3\text{Fe}_5(\text{CO}_3)_3\text{O}_9 \rightarrow \text{Y}_3\text{Fe}_5(\text{CO}_3)\text{O}_{11}$  (661.9–803 K,  $T_{\max \text{DTG}}=728$  K, calcd./found: 3.56/3.39%)  $\rightarrow \text{Y}_3\text{Fe}_5(\text{CO}_3)_0.5\text{O}_{11.5}$  (948.6–1033.8 K, calcd./found: 0.89/0.78%)  $\rightarrow \text{Y}_3\text{Fe}_5\text{O}_{12}$  (1054.8–1160.8 K, calcd./found: 0.89/0.83%). The presence of the carbonate anion is confirmed by FTIR analysis of the reaction intermediate

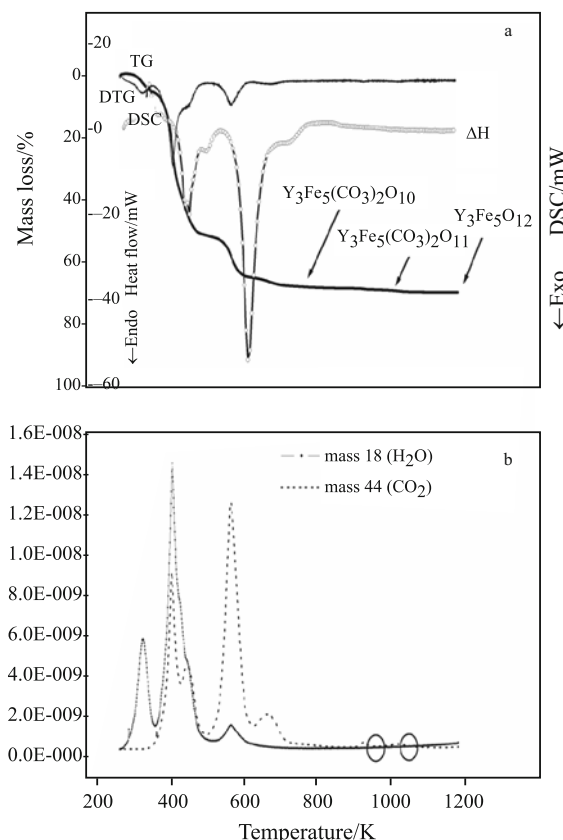


**Fig. 1** a – TG, DTG, DSC, and b – ion intensities curves  $m/z=18$  ( $\text{H}_2\text{O}$ ) and 44 ( $\text{CO}_2$ ) of the polynuclear coordination compound  $(\text{NH}_4)_6[\text{Y}_3\text{Fe}_5(\text{C}_4\text{O}_5\text{H}_4)_6(\text{C}_4\text{O}_5\text{H}_3)_6]\cdot 12\text{H}_2\text{O}$  (heating rate=5°C min<sup>-1</sup>)

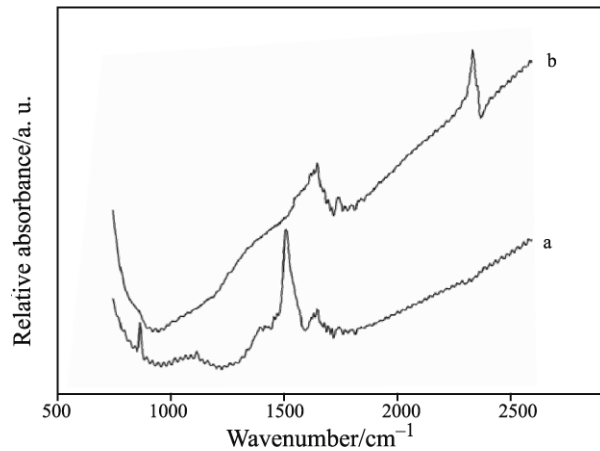


**Fig. 2** IR spectra of a –  $(\text{NH}_4)_6[\text{Y}_3\text{Fe}_5(\text{C}_4\text{O}_5\text{H}_4)_6(\text{C}_4\text{O}_5\text{H}_3)_6]\cdot 12\text{H}_2\text{O}$  and b –  $(\text{NH}_4)_6[\text{Y}_3\text{Fe}_5(\text{C}_6\text{O}_7\text{H}_{10})_6(\text{C}_6\text{O}_7\text{H}_9)_6]\cdot 8\text{H}_2\text{O}$  decomposition intermediates isolated at 500°C

(Fig. 2). The carbonate characteristic absorption peaks are detected at:  $\sim 1550$ ,  $\sim 1390$  (attributed to the split anti-symmetrical carbonate stretching) and  $\sim 850\text{ cm}^{-1}$  (attributed to the out of plane bending of carbonate).

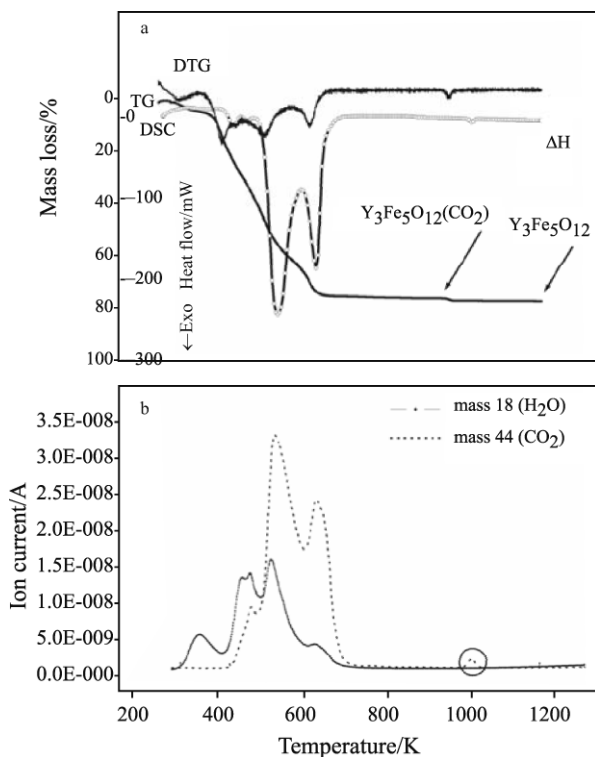


**Fig. 3** a – TG, DTG, DSC, and b – ion intensities curves  $m/z=18$  ( $\text{H}_2\text{O}$ ) and  $44$  ( $\text{CO}_2$ ) of the polynuclear coordination compound  $(\text{NH}_4)_6[\text{Y}_3\text{Fe}_5(\text{C}_6\text{O}_7\text{H}_{10})_6(\text{C}_6\text{O}_7\text{H}_9)_6]\cdot 8\text{H}_2\text{O}$  (heating rate =  $5^\circ\text{C min}^{-1}$ )

For the gluconate coordination compound  $(\text{NH}_4)_6[\text{Y}_3\text{Fe}_5(\text{C}_6\text{O}_7\text{H}_{10})_6(\text{C}_6\text{O}_7\text{H}_9)_6]\cdot 8\text{H}_2\text{O}$  six decomposition mass losses are evidenced in the temperature range of 316.3–1050.2 K (Fig. 3). The experimental and the theoretical mass losses assuming  $\text{Y}_3\text{Fe}_5\text{O}_{12}$  formation are close (calcd./found: 76.34/76.39%). The TG, DSC, DTG and  $m/z=18$  ( $\text{H}_2\text{O}$ ) and  $44$  ( $\text{CO}_2$ ) curves are presented in Fig. 3.

The first step (316.3–417 K,  $T_{\max \text{ DTG}}=342.8$  K) represents the endothermic release of six ammonia and two water molecules (calcd./found: 4.42/4.31%). The next four decomposition stages (417–480.8 K,  $T_{\max \text{ DTG}}=355.7$  K; 480.8–507 K,  $T_{\max \text{ DTG}}=493.6$  K; 507–627.4 K,  $T_{\max \text{ DTG}}=562.9$  K; 627.4–735.8 K,  $T_{\max \text{ DTG}}=672.4$  K) associated with exothermic effects represent the oxidative degradation of the ligand. Their thermal stoichiometry can not be established due to the partially overlapping processes. The corresponding mass losses are: 23.96, 8.57, 29.74 and 8.4% and the main evolved gaseous products are  $\text{CO}_2$  and  $\text{H}_2\text{O}$ . The formed reaction intermediate may be formulated as an oxide (amorphous as resulted from X-ray investigations) containing entrapped  $\text{CO}_2$ , with the molecular formula  $\text{Y}_3\text{Fe}_5\text{O}_{12}(\text{CO}_2)$ . The above formulation is sustained by the following experimental

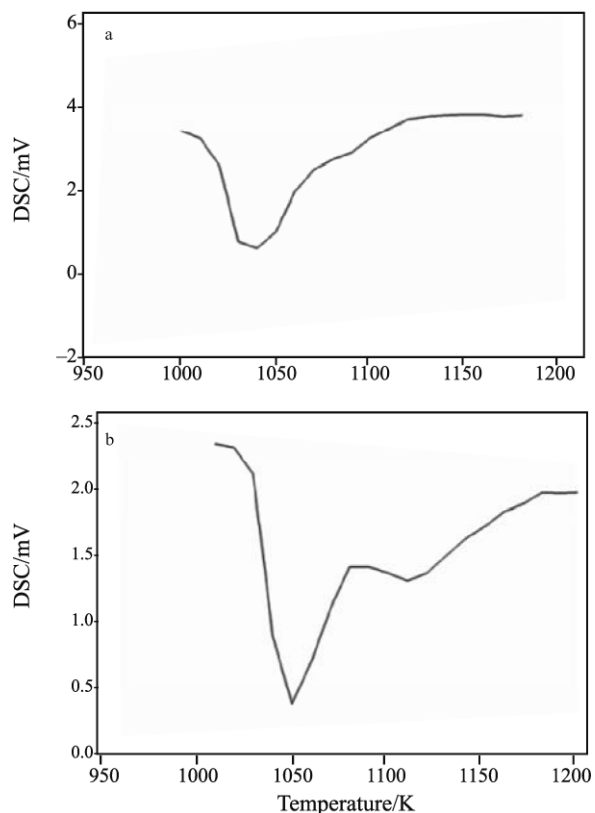


**Fig. 4** DSC curves registered for  
a –  $(\text{NH}_4)_6[\text{Y}_3\text{Fe}_5(\text{C}_6\text{O}_7\text{H}_{10})_6(\text{C}_6\text{O}_7\text{H}_9)_6]\cdot 8\text{H}_2\text{O}$  and  
b –  $(\text{NH}_4)_6[\text{Er}_3\text{Fe}_5(\text{C}_6\text{O}_7\text{H}_{10})_6(\text{C}_6\text{O}_7\text{H}_9)_6]\cdot 22\text{H}_2\text{O}$  compounds (heating rate  $20^\circ\text{C min}^{-1}$ )

results: (i) the stoichiometric results (mass loss calcd./found.=70.51/70.67%) (ii) the presence in the FTIR spectrum of the intermediate isolated at 773 K of an absorption peak at  $2350\text{ cm}^{-1}$ , characteristic to the trapped  $\text{CO}_2$  [22] and the absence of the  $\text{CO}_3^{2-}$  typical absorption bands. The formed decomposition intermediate decomposes in the temperature range 1020.3–1050.2 K ( $T_{\max \text{ DTG}}=1030.5$  K) with the elimination of one  $\text{CO}_2$  molecule, stoichiometry sustained from both thermogravimetric and mass spectrometry calculation (calcd./found.=1.41/1.38%). This decomposition process is associated with an overall exothermic process, which suggests that the endothermic elimination of  $\text{CO}_2$  is accompanied or has as effect structural rearrangements such as crystallization. The exothermic effect associated to the structural rearrangements prevails in comparison with the endothermic release of  $\text{CO}_2$ . Performing experiments with high heating rates ( $20\text{ K min}^{-1}$ ), it was possible to discriminate the existence of the two processes attributed to  $\text{CO}_2$  elimination and structural rearrangements. The obtained DSC curve (Fig. 4a) evidenced two thermal effects the first at 1050.9 K and the second as a shoulder at ~1091 K. The TEM investigations (Fig. 5) of the final decomposition

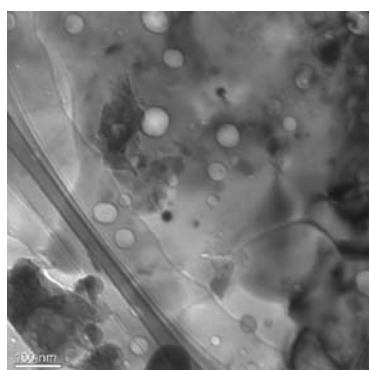


**Fig. 5** TEM image of the product resulted from  $(\text{NH}_4)_6[\text{Y}_3\text{Fe}_5(\text{C}_6\text{O}_7\text{H}_{10})_6(\text{C}_6\text{O}_7\text{H}_9)_6]\cdot 8\text{H}_2\text{O}$  decomposition

products reveal the existence of spherical voids (with diameters up to 50 nm) characteristic for entrapped gases evolving.

#### *Er-Fe coordination compounds thermal decomposition*

The thermal decomposition of the coordination compound  $(\text{NH}_4)[\text{Er}_3\text{Fe}_5(\text{C}_4\text{O}_5\text{H}_4)_6(\text{C}_4\text{O}_5\text{H}_3)_6]\cdot 10\text{H}_2\text{O}$  occurs in the temperature range of 325.8–1002.5 K. The registered experimental loss is 63.76% in comparison with the theoretical one 63.24% assuming  $\text{Er}_3\text{Fe}_5\text{O}_{12}$  formation as the final product. The TG, DTG, DSC and  $m/z=18$  ( $\text{H}_2\text{O}$ ) and 44 ( $\text{CO}_2$ ) curves are depicted in Fig. 6.

The decomposition starts (325.8–417 K,  $T_{\max \text{ DTG}}=367$  K) with the endothermic evolving of 6 $\text{NH}_3$  and 2 $\text{H}_2\text{O}$  molecules (calcd./found: 5.28/4.50%). The second process occurs at 417–562.8 K, ( $T_{\max \text{ DTG}}=478$  K). Besides the evolving of the remainder water molecules, the decomposition of the organic ligand occurs. As in the case of yttrium-iron malate coordination compound, the formation of an oxoacetate decomposition intermediate corresponding to the  $\text{Er}_3\text{Fe}_5\text{O}_6(\text{CH}_3\text{COO})_{12}$  (calcd./found: 34.84/34.48%) may be advanced. The same absorption peaks characteristic to acetate anion are presented in the FTIR spectrum of the above mentioned intermediate. Further, the intermediate decomposes in the temperature range of 562.8–652.4 K, leading to the formation of the oxocarbonate  $\text{Er}_3\text{Fe}_5(\text{CO}_3)_4\text{O}_8$  (calcd./found: 16.47/17.56%). Further, a two-stepped decomposition of  $\text{Er}_3\text{Fe}_5(\text{CO}_3)_4\text{O}_8$  to  $\text{Er}_3\text{Fe}_5\text{O}_{12}$  via  $\text{Er}_3\text{Fe}_5(\text{CO}_3)_2\text{O}_{10}$  occurs at 652.4–1002.5 K, (652.4–802.4 K,  $T_{\max \text{ DTG}}=737.4$  K; 952.4–1002.5 K,  $T_{\max \text{ DTG}}=987$  K; calcd./found: 3.32/3.62%; calcd./found: 3.32/3.18%). The single gaseous product detected during the two last processes is  $\text{CO}_2$ .

Thermal decomposition of the gluconate compound,  $(\text{NH}_4)_6[\text{Er}_3\text{Fe}_5(\text{C}_6\text{O}_7\text{H}_{10})_6(\text{C}_6\text{O}_7\text{H}_9)_6]\cdot 22\text{H}_2\text{O}$  which occurs in the range of 330–1113 K

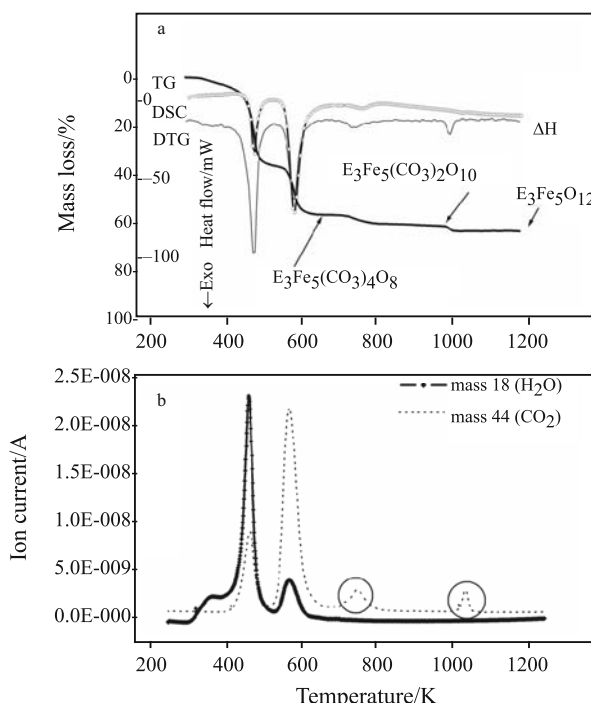


**Fig. 6** a – TG, DTG, DSC, and b – ion intensities curves  $m/z=18$  ( $\text{H}_2\text{O}$ ) and 44 ( $\text{CO}_2$ ) of the polynuclear coordination compound  $(\text{NH}_4)_6[\text{Er}_3\text{Fe}_5(\text{C}_4\text{O}_5\text{H}_4)_6(\text{C}_4\text{O}_5\text{H}_3)_6]\cdot 10\text{H}_2\text{O}$  (heating rate=5°C min<sup>-1</sup>)

leads to the formation of a final product with formula  $\text{Er}_3\text{Fe}_5\text{O}_{12}$  (calcd./found: 73.02/73.16%). The TG, DSC, DTG and  $m/z=18$  ( $\text{H}_2\text{O}$ ) and 44 ( $\text{CO}_2$ ) curves are presented in Fig. 7.

The evolving of the 6 $\text{NH}_3$  and  $\text{H}_2\text{O}$  molecules (calcd./found: 5.82/5.81% represents the first decomposition step (330–392.3 K). The next decomposition stage (392.3–742.4 K) associated with exothermic effects, represents besides the elimination of the remainder water molecules (the peak from 187°C on  $m/z=18$  curve) the oxidative degradation of the ligand. Three peaks were identified on both DTG and DSC curves ( $T_{\max \text{ DTG}}=484.6$ , 552.9 and ~597 K,  $T_{\max \text{ DSC}}=484.5$ , 558.8 and 602.5 K). The shape of both curves are characteristic for overlapping processes. The decomposition intermediate isolated at 773 K corresponds to the molecular formulation  $\text{Er}_3\text{Fe}_5\text{O}_{12}(\text{CO}_2)$  (calcd./found: 65.99/65.28%), being amorphous from crystallographic point of view. Similar to the intermediate obtained from yttrium-iron gluconate compound, the FTIR spectrum of  $\text{Er}_3\text{Fe}_5\text{O}_{12}(\text{CO}_2)$  intermediate presents an absorption peak at 2350 cm<sup>-1</sup>, characteristic to the trapped  $\text{CO}_2$ . The last decomposition step (1012.5–1042.5 K) corresponds to the evolving of the remainder  $\text{CO}_2$  molecules and the formation of  $\text{Er}_3\text{Fe}_5\text{O}_{12}$  garnet (calcd./found: 1.21/1.12%). As in the case of analogous yttrium compound, two processes

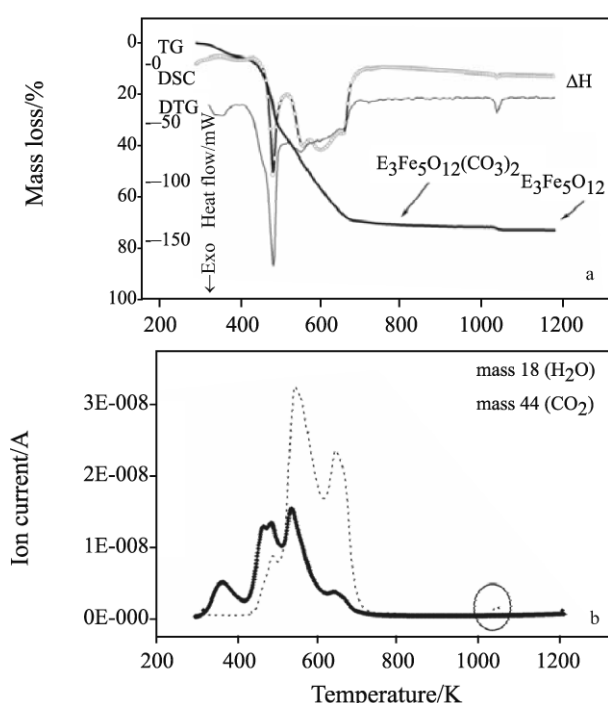


**Fig. 7** a – TG, DTG, DSC, and b – ion intensities curves  $m/z=18$  ( $H_2O$ ) and 44 ( $CO_2$ ) of the polynuclear coordination compound  $(NH_4)_6[Er_3Fe_5(C_6O_7H_{10})_6(C_6O_7H_9)_6]\cdot22H_2O$  (heating rate=5°C min<sup>-1</sup>)

were identified on the DSC curve the Fig. 4b, corresponding to  $CO_2$  and structural rearrangements.

#### Mixed oxide characterization

The X-ray analysis of the oxides obtained by the decomposition of the four coordination compounds reveals the following:

- The thermal decompositions of both malate compounds generate at 973–1073 K a mixture of simple ( $Y_2O_3$ ,  $Er_2O_3$ ,  $Fe_3O_4$ ,  $\alpha$ - and  $\gamma$ - $Fe_2O_3$ ) and mixed ( $YFeO_3$ ,  $ErFeO_3$  and  $Er_3Fe_5O_{12}$ ) oxides. While in the case of the product derived from yttrium-iron malate compound  $Y_3Fe_5O_{12}$  crystallizes only in small amounts, at temperatures higher than 1173 K, in the decomposition products obtained from erbium-iron malate compound, the garnet represents the majority phase. The mean crystallite sizes of yttrium and erbium garnets obtained at 1173 K are 335 respectively, 455 Å.
- The thermal decompositions of yttrium-iron and erbium-iron gluconate compounds lead to the obtaining of pure garnets ( $Y_3Fe_5O_{12}$  and  $Er_3Fe_5O_{12}$ ) at 1073 K (Fig. 8). The mean crystallite sizes of yttrium and erbium garnets obtained at 1073 K are 430 and 300 Å, respectively.

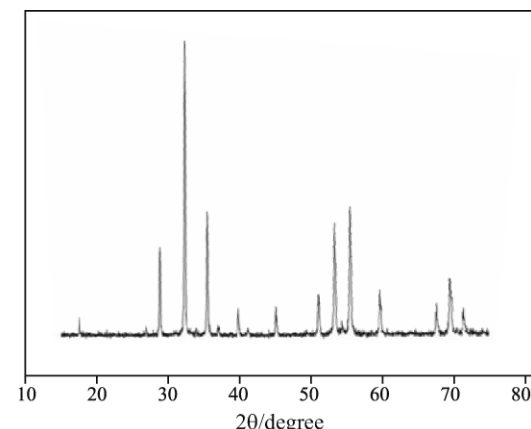


**Fig. 8** X-ray diffraction pattern of the  $Y_3Fe_5O_{12}$  obtained from gluconate compound at 800°C (1 h calcination time)

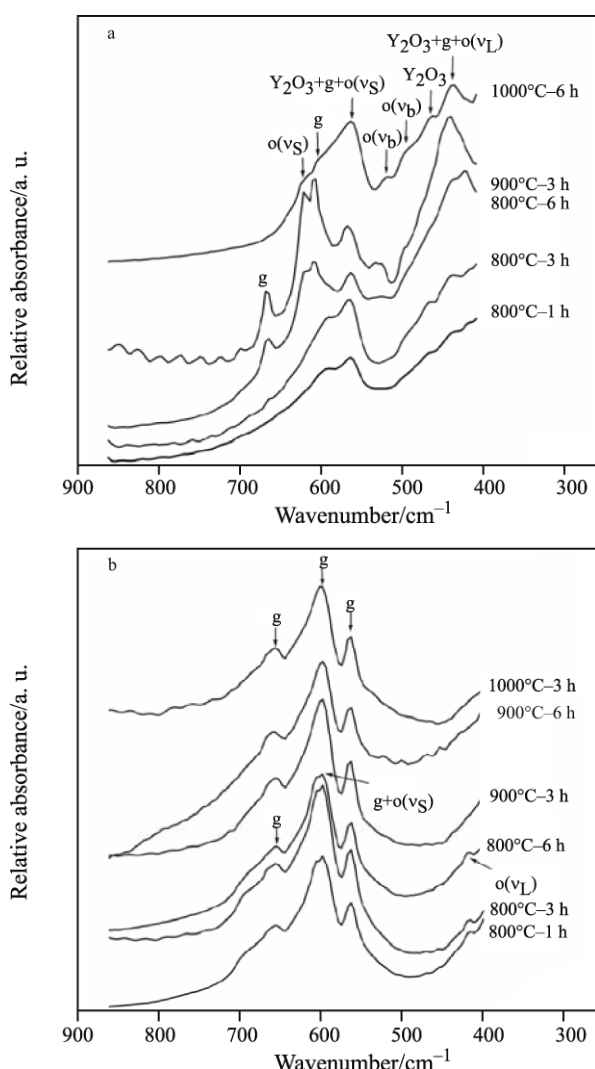


**Fig. 9** FTIR spectra of the end products obtained by decomposition of  
a –  $(NH_4)_6[Y_3Fe_5(C_4O_5H_4)_6(C_4O_5H_3)_6]\cdot12H_2O$  and  
b –  $(NH_4)_6[Y_3Fe_5(C_6O_7H_{10})_6(C_6O_7H_9)_6]\cdot8H_2O$  coordination compounds (heating rate 5°C min<sup>-1</sup>)

The infrared absorption spectra of the final products obtained from the four polynuclear coordination compounds after various thermal treatments confirmed the X-ray experiments. As example, we mention only the case of yttrium–iron coordination compounds (Fig. 9). The FTIR spectrum of the yttrium garnet  $\text{Y}_3\text{Fe}_5\text{O}_{12}$ , is characterized by the presence of three bands at 660, ~600 and ~565  $\text{cm}^{-1}$  assigned to the stretching mode of the tetrahedral coordinated cations [23, 24]. The FTIR spectrum of the oxide obtained from malate precursor exhibits also the bands characteristic to the orthorhombic ferrite, attributed to the stretching ( $\nu_s$ , 560–620  $\text{cm}^{-1}$ ), bending ( $\nu_b$ , 540–520  $\text{cm}^{-1}$ ) and lattice ( $\nu_L$ ~420  $\text{cm}^{-1}$ ) vibrations, the first two ones splitted. Typical bands of  $\text{Y}_2\text{O}_3$  (~560, ~460 and ~420  $\text{cm}^{-1}$ ) are as well detected.

## Conclusions

Both, the thermal behaviour of the investigations coordination compounds and the phase compositions of the resulted decomposition products depend on the nature of metallic cations (yttrium–iron or erbium–iron) and ligand anions (malate or gluconate).

The following conclusions may be pointed out:

- The thermal degradations of the malate coordination compounds occur in well defined steps, via an amorphous oxoacetate and two amorphous oxocarbonate intermediates. The phase composition of the final decomposition products consists in a mixture of simple ( $\text{Y}_2\text{O}_3$ ,  $\text{Er}_2\text{O}_3$ ,  $\text{Fe}_3\text{O}_4$ ,  $\alpha$ - and  $\gamma$ - $\text{Fe}_2\text{O}_3$ ) and mixed ( $\text{YFeO}_3$ ,  $\text{ErFeO}_3$ ,  $\text{Y}_3\text{Fe}_5\text{O}_{12}$  and  $\text{Er}_3\text{Fe}_5\text{O}_{12}$ ) oxides. The increase of the temperature determines the formation of mixed oxides: in the case of yttrium–iron malate compound the orthorhombic  $\text{YFeO}_3$  is preferentially formed, while in the case of erbium–iron malate compound the cubic  $\text{Er}_3\text{Fe}_5\text{O}_{12}$  is obtained.
- The decomposition steps of the gluconate compounds are partially overlapped. The intermediates isolated at the end of the anionic ligand degradation, are amorphous oxides with entrapped  $\text{CO}_2$ . These entrapped gases are released only when the ordering during crystallization occurs, fact which determines the obtaining of pure garnet oxide products simultaneously with the decomposition process.

## References

- 1 O. Carp and E. Segal, Rev. Roum. Chim., 39 (1994) 1123.
- 2 M. Brezeanu, L. Patron and M. Andruh, Polynuclear Coordination Compounds and their Application, Ed. Academiei 1986.
- 3 I. Mindru, L. Patron and M. Brezeanu, Roum. Chem. Quart. Rev., 4 (1996) 167.
- 4 P. E. Rush, J. D. Oliver, G. D. Simpson and G. O. Carlisle, J. Inorg. Nucl. Chem., 37 (1975) 1393.
- 5 S. Kirschner and A. Kiesling, J. Am. Chem. Soc., 20 (1960) 4174.
- 6 N. Dennis Chasteen and R. Linn Belford, Inorg. Chem., 9 (1970) 169.
- 7 I. Valiuna and K. P. Pribyl, Russ. J. Inorg. Chem., 36 (1991) 379.
- 8 B. S. Randhawa and K. J. Sweety, J. Therm. Anal. Cal., 65 (2001) 829.
- 9 S. Sarmah and N. N. Dass, J. Thermal Anal., 54 (1988) 913.
- 10 N. Deb, J. Therm. Anal. Cal., 78 (2004) 237.
- 11 N. N. Mallikarjuna, A. Lagashetty and A. Venkataraman, J. Therm. Anal. Cal., 74 (2003) 819.
- 12 V. Logvinenko, L. Yudanova, N. Yudanov and G. Chekhova, J. Therm. Anal. Cal., 74 (2003) 395.
- 13 D. G. Karraker, Inorg. Chem., 6 (1967) 1863.
- 14 D. G. Karraker, Inorg. Chem., 7 (1967) 473.
- 15 K. Nakamoto, Infrared and Raman Spectra of Inorganic and Coordination Compounds, 4<sup>th</sup> Ed., J. Wiley & Sons, 1986.
- 16 L. Patron, O. Carp, I. Mindru, G. Marinescu, N. Stanica and I. Balint, J. Serb. Chem. Soc., 70 (2005) 1049.
- 17 P. Baraldi, Spectrochim. Acta, 38 (1982) 51.
- 18 O. Carp, L. Patron, I. Mindru, G. Marinescu, L. Diamandescu and A. Banuta, J. Therm. Anal. Cal., 74 (2003) 789.
- 19 O. Carp, L. Patron, E. Segal, R. Barjega and M. Brezeanu, J. Therm. Anal. Cal., 56 (1999) 513.
- 20 I. Mindru, L. Patron, O. Carp, G. Marinescu, M. Pascu, G. Pascu and L. Diamandescu, Rev. Roum. Chim., 49 (2004) 235.
- 21 M. A. Mohamed, A. K. Galwey and S. Halawy, Thermochim. Acta, 323 (1998) 27.
- 22 A. C. Tass, P. J. Majewski and F. Aldinger, J. Am. Ceram. Soc., 83 (2000) 2954.
- 23 A. M. Hofmeister and K. R. Campbell, J. Appl. Phys., 72 (1992) 638.
- 24 M. Ristic, I. Nowik, S. Popovic, I. Feluer and S. Music, Mater. Lett., 57 (2003) 2584.

---

DOI: 10.1007/s10973-007-8839-4